PERGAMON

Aerosol Science 34 (2003) 691–711

Journal of
Aerosol Science

www.elsevier.com/locate/jaerosci

An experimental and numerical study of particle nucleation and growth during low-pressure thermal decomposition of silane

Sandeep Nijhawan[a,1], Peter H. McMurry[a,*], Mark T. Swihart[a,2], Song-Moon Suh[a], Steven L. Girshick[a], Stephen A. Campbell[b], John E. Brockmann[c]

[a] *Department of Mechanical Engineering, University of Minnesota, 111 Church St. SE, Minneapolis, MN 55455, USA*
[b] *Department of Electrical Engineering, University of Minnesota, 200 Union St. SE, Minneapolis, MN 55455, USA*
[c] *Sandia National Laboratory, Department 9114, MS 0827, Albuquerque, NM 87185, USA*

Received 1 June 2002; accepted 16 January 2003

Abstract

This paper discusses an experimental and numerical study of the nucleation and growth of particles during low-pressure (~1.0 Torr) thermal decomposition of silane (SiH_4). A Particle Beam Mass Spectrometer was used to measure particle size distributions in a parallel-plate showerhead-type semiconductor reactor. An aerosol dynamics moment-type formulation coupled with a chemically reacting fluid flow model was used to predict particle concentration, size, and transport in the reactor. Particle nucleation kinetics via a sequence of chemical clustering reactions among silicon hydride molecular clusters, growth by heterogeneous chemical reactions on particle surfaces and coagulation, and transport by convection, diffusion, and thermophoresis were included in the model. The effect of pressure, temperature, flow residence time, carrier gas, and silane concentration were examined under conditions typically used for low-pressure (~1 Torr) thermal chemical vapor deposition of polysilicon. The numerical simulations predict that several pathways involving linear and polycyclic silicon hydride molecules result in formation of particle "nuclei," which subsequently grow by heterogeneous reactions on the particle surfaces. The model is in good agreement with observations for the pressure and temperature at which particle formation begins, particle sizes and growth rates, and relative particle concentrations at various process conditions. A simplified, computationally inexpensive, quasi-coupled modeling approach is suggested as an engineering tool for process equipment design and contamination control during low-pressure thermal silicon deposition.

* Corresponding author. Tel.: +1-612-624-2817; fax: +1-612-626-1854.
E-mail address: mcmurry@me.umm.edu (P.H. McMurry).
[1] Present Address: Applied Materials, Bowers Avenue, Santa Clara, CA 95054, USA.
[2] Present Address: Department of Chemical Engineering, University of Buffalo (SUNY), Buffalo, NY 14260, USA.

0021-8502/03/$ - see front matter
doi:10.1016/S0021-8502(03)00029-6

1. Introduction

Particle contamination control has been recognized as the key to maintaining profitability in high-end semiconductor manufacturing. A conservative estimate shows that more than half of the product yield losses in semiconductor manufacturing are from particle-induced defects (Hattori, 1990). O'Hanlon and Parks (1992) note that the primary source of contamination during manufacturing is particle generation within the process equipment. Furthermore, as the semiconductor device features are rapidly shrinking, there is an increasing interest in ultrafine (< 0.1 μm) particle contamination control. The 2001 International Technology Roadmap for Semiconductor projects that by the year 2004 deposition of particles larger than 0.045 μm will lead to yield losses. Such small particles are typically generated by homogeneous nucleation and growth during processing, indicating the importance of these processes in semiconductor manufacturing. In this paper we present a model for particle nucleation and growth in low-pressure chemical vapor deposition (CVD) of polysilicon from silane, a commonly used semiconductor manufacturing process, and compare the model predictions to experimental results.

Various mechanisms for particle nucleation during thermal CVD of polysilicon from silane (SiH_4) have been proposed. Several researchers suggest formation of supersaturated silicon vapor in the gas phase as the driving force for nucleation during silane pyrolysis (Flint, Marra, & Haggerty, 1986; Herrick & Martinez, 1984a; Herrick & Woodruff, 1984b; Allen & Sawin, 1986; Kruis, Schoonman, & Scarlett, 1994; Kelkar, Rao, & Girshick, 1996). However, such models do not account for the experimental observation that particles formed during silane pyrolysis contain hydrogenated silicon groups rather than coalesced bulk silicon (Purnell & Walsh, 1966; Onischuk, Strunin, Ushakova, & Panfilov, 1994; Onischuk et al., 1997a; Onischuk, Strunin, Ushakova, & Panfilov, 1997b; Frenklach, Ting, Wang, & Rabinowitz, 1996). To account for hydrogen in particles, polymerization reaction pathways involving successive insertion of reactive species in linear polysilanes have been proposed (Brekel & Bollen, 1981; White, Espino-Rios, Rogers, Ring, & O'Neal, 1985; Yuuki, Matsui, & Tachibana, 1987; Giunta, McCurdy, Chapple-Sokol, & Gordon, 1990; Frenklach et al., 1996). In contrast, Veprek, Schopper, Ambacher, Rieger, and Veprek-Heijman (1993) and Ho, Nijhawan, and Brockmann (1996) have argued that since linear polysilanes can easily dissociate by SiH_2 or H_2 elimination, they cannot explain the formation of stable particle "nuclei" in the gas phase that are more likely to grow than to decay. These authors postulated the importance of cyclic polysilanes in nucleation kinetics, as they are thermally stable and thus once formed are likely to grow irreversibly. Recently, Girshick and coworkers developed a chemical kinetic nucleation model in which linear and cyclic silicon hydride species containing up to 10 silicon atoms were considered. Several chemical clustering pathways involving polycyclic species were identified as rate-limiting bottlenecks under atmospheric pressure conditions (Swihart & Girshick, 1999a, b).

Once a stable nucleus is formed, subsequent growth can occur by Brownian coagulation and (physical or chemical) adsorption of gas phase species on the cluster surface. Sladek (1971) proposed a collision-limited particle growth model in CVD applications. However, for typical flow residence times in low-pressure CVD reactors (< 1 s), coagulation cannot explain the measured particle concentration ($< 10^7$ cm^{-3}) and growth rate (~ 0.1 μm/s) reported in the literature and this work.

Although, it is firmly established that surface kinetics plays an important role during film growth on a hot silicon surface (Joyce & Bradley, 1963; Brekel & Bollen, 1981; Claassen, Bloem, Valkenburg, & van den Brekel, 1982; Donahue & Reif, 1986; Foster, Learn, & Kamins, 1986; Buss, Ho,

Breiland, & Coltrin, 1988; Comfort & Reif, 1989), the precise role of heterogeneous chemistry on particle surfaces has been debated in the literature. Eversteijn (1971) notes that under atmospheric pressure conditions with hydrogen as carrier gas, the activation energy for particle formation ($\sim$ 38 kcal/mole) is close to the activation energy of silane adsorption on silicon ($\sim$ 30–40 kcal/mole) indicating that heterogeneous decomposition of silane on particle surfaces is the rate-limiting step during particle formation. However, this explanation is not applicable to particle formation under atmospheric-pressure conditions in inert carrier gases, where activation energies of the order of 130 –150 kcal/mol have been reported (Slootman & Parent, 1994). Recently, Onischuk et al. (1997b) showed that in atmospheric-pressure silane decomposition, heterogeneous growth rates from linear saturated polysilanes (like silane, disilane, trisilane, etc.) are roughly a factor of 100 lower than the measured particle growth rates adding to the debate on the role of heterogeneous chemistry during particle growth.

In this work we present particle measurements under low-pressure conditions ($\sim$1 Torr) in a parallel-plate reactor and compare the experimental results to 1D, steady state, stagnation flow numerical simulations. The numerical model includes relevant thermal processes such as particle nucleation via chemical-clustering reactions, particle growth via heterogeneous surface reactions and coagulation, and transport. Numerical results using both fully coupled and quasi-coupled formulations are presented. We refer the reader to Nijhawan (1999) for detailed derivation of the model and Girshick, Swihart, Suh, Mahajan, and Nijhawan (2000) for details of the chemical clustering kinetics in silane pyrolysis.

2. Experimental

Fig. 1 shows the schematic of the experimental setup. We used a modified Gaseous-Electronics Conference (GEC) reference cell process reactor (Hargis et al., 1994; Nijhawan, 1999). Process gases entered through a showerhead inlet and exited through a series of annular slots in the lower flange of the process chamber. A wafer was mounted on a heated substrate at a distance of 6.8 cm from the showerhead inlet. Particle measurements were made using the PBMS (Ziemann, Liu, Rao, Kittelson, & McMurry, 1995a). The PBMS is an extractive sampling technique in which the sampled flow passes through a series of "aerodynamic lenses" to form a tightly collimated particle beam (Liu, Ziemann, Kittelson, & McMurry, 1995a,b). Using a nozzle-skimmer assembly, the particle beam is transported with nearly 100% efficiency to a high-vacuum chamber ($< 10^{-5}$ Torr), where the particles are charged to saturation by electron impact and classified using a 90° electrostatic deflector based on the kinetic energy-to-charge ratio. Based on the previously obtained particle Stokes number-velocity (Liu et al., 1995b; Nijhawan, 1999) and particle diameter-charge calibrations (Ziemann et al., 1995a; Ziemann, Kittelson, & McMurry, 1996) quantitative particle size distributions are obtained in the 0.02 to $\sim$0.5 μm diameter range. We have previously demonstrated this technique by measuring particles in thermal (Ziemann et al., 1995a; McMurry et al., 1996; Nijhawan et al., 1998; Rao et al., 1998a) and plasma enhanced (Rao et al., 1998b) CVD processes. It should be noted that due to an almost linear particle diameter-charge calibration the PBMS is capable of obtaining useful information on particles as small as 0.005 μm (Ziemann et al., 1995b). However, for such small particles considerable uncertainty exists in determining particle number concentration due to transport losses, which increase sharply with decreasing size below 0.02 μm.

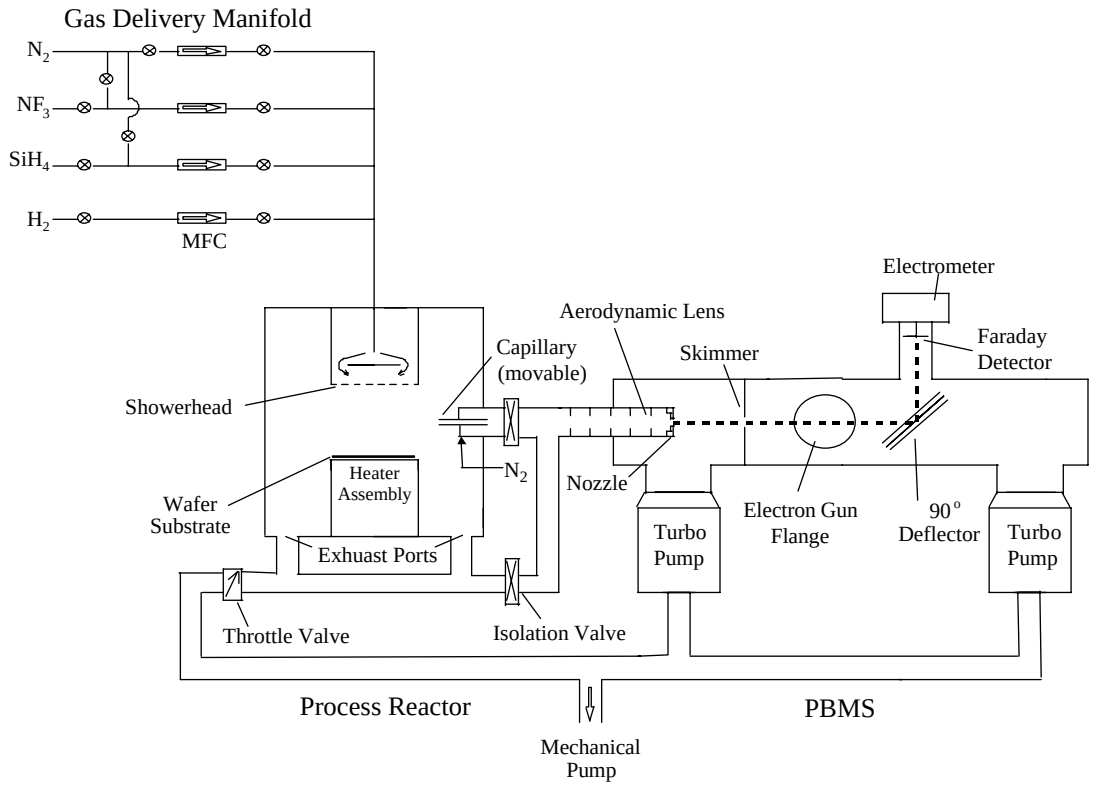

Fig. 1. Schematic diagram of the experimental setup.

In this work PBMS measurements from within the process reactor and the exhaust line are presented. No special sampling inlet was used for exhaust-line measurements. However, a capillary inlet as shown in Fig. 1 was used to withdraw localized samples from within the process reactor. To minimize any distortion to the fluid flow in the parallel-plate region of the reactor, the capillary inlet samples less than 2% of the total flow introduced at the showerhead inlet along a radial plane located at the exit of the parallel-plate region. The aerosol sampled by the capillary was diluted with annular nitrogen sheath (1) to make up for the flow requirements of the PBMS, (2) to quench any chemical reactions in the hot process gases, and (3) to increase particle transport by confining the particles along the centerline. We refer the reader to Nijhawan (1999) for details of the capillary probe design.

3. Modeling

Fig. 2 shows a schematic diagram of the modeling components and their interrelationships. Briefly, conservation equations of total mass, momentum, species mass, and energy were solved to predict the steady-state chemically reacting incompressible, laminar, non-isothermal flow-field between the showerhead and wafer substrate region of the reactor. The 2D-axisymmetric governing equations are transformed to 1D using the self-similar stagnation flow transformation (Coltrin, Kee, & Miller,

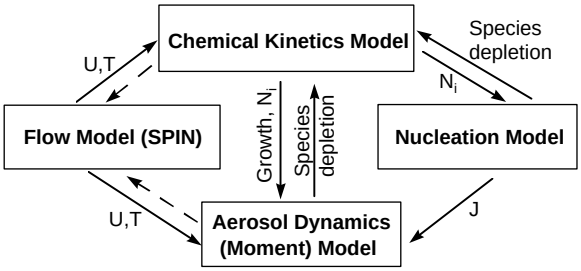

Fig. 2. Schematic diagram of the various modeling components and their relationships to each other. In the figure U, T, N_i, and J refer to the velocity, temperature, species number concentration, and nucleation rate, repectively. (Dashed arrows indicate a weak coupling.)

1986; Coltrin et al., 1991). Although this similarity solution is strictly applicable only to a stagnation flow field with infinite radial extent, detailed 2D fluid flow modeling indicates that it is a good approximation within one-half radius of the wafer substrate (Nijhawan, 1999). The dynamic behavior of the aerosol is modeled by solving the continuous aerosol general dynamic equation (GDE) using the method of moments assuming a lognormal size distribution function (Pratsinis & Kim, 1989; Phanse & Pratsinis, 1989; Whitby, 1990; Chiu, 1992). Due to the small particle size of interest, particle inertia is neglected and free-molecular regime expressions based on Epstein's (1924) slip correction are used to describe particle transport. Also, molecular clusters and particles are assumed to be in thermal equilibrium with the surrounding gas following ideal gas laws. Gas phase concentrations of molecular clusters are determined from the chemical species mass conservation equations, while particle size distributions (including particle nuclei) are determined by solving the moment form of the aerosol GDE. Particle growth by coagulation and heterogeneous surface reactions is included in the model.

The transformed 1D axisymmetric chemically reacting fluid flow equations were solved using the commercially available code SPIN (Coltrin, et al., 1991) version 5.15. SPIN evaluates finite rate gas phase and surface chemistry using the CHEMKIN family of codes (Kee, Rupley, Meeks, & Miller, 1996; Coltrin, Kee, Rupley, & Miller, 1996) and is thus ideally suited for solving nucleation kinetics and aerosol dynamics in chemically reacting stagnation-point flows. The SPIN software code was modified to include other modeling components shown in Fig 2. Note that the model fully couples the gas phase and aerosol dynamics. That is, the gas phase species mass conversation equation was modified to include terms that account for species depletion due to particle formation and growth. Furthermore the equation of state was modified to account for thermodynamic pressure exerted by particles in analogy to the partial pressure exerted by any gas phase species. We refer the reader to Nijhawan (1999) for a detailed description and derivation of the governing equations. The specific aspects of the model relevant to nucleation and growth during silane pyrolysis and the numerical algorithm used in this work are discussed below.

3.1. Homogeneous kinetics model and nucleation rate

Particle nucleation was modeled using the silicon hydride clustering mechanism of Swihart and Girshick (1999a). A total of 469 reversible reactions among 106 silicon hydride species containing

Table 1
Reversible gas phase chemical clustering reactions of Swihart and Girshick (1999a) used in this study.

	Reaction type	Prototypical reactions	General form
R1	H_2 elimination from a saturated polysilane	$SiH_4 \rightleftharpoons SiH_2 + H_2$ $Si_2H_6 \rightleftharpoons Si_2H_4B + H_2$	$Si_nH_{2m} \rightleftharpoons Si_nH_{2m-2}B + H_2$
R2	Silylene elimination from a saturated polysilane	$Si_2H_6 \rightleftharpoons SiH_2 + SiH_4$ $Si_3H_8 \rightleftharpoons Si_2H_4B + SiH_4$	$Si_nH_{2m} \rightleftharpoons Si_lH_{2k}B + Si_{n-l}H_{2(m-k)}$
R3	Silylene elimination from a silene	$Si_3H_6A \rightleftharpoons SiH_2 + Si_2H_4A$ $Si_4H_8A \rightleftharpoons Si_2H_4B + Si_2H_4A$	$Si_nH_{2m}A \rightleftharpoons Si_lH_{2k}B + Si_{n-l}H_{2(m-k)}A$
R4	Silylene to silene isomerization	$Si_2H_4B \rightleftharpoons Si_2H_4A$ $Si_3H_6B \rightleftharpoons Si_3H_6A$	$Si_nH_{2m}B \rightleftharpoons Si_nH_{2m}A$
R5	Ring addition	$Si_3H_6B \rightleftharpoons Si_3H_6$ $Si_4H_8B \rightleftharpoons Si_4H_8$	$Si_nH_{2m}B \rightleftharpoons Si_nH_{2m}$

ten or fewer silicon atoms was included in this model. For each silicon hydride molecule, the most stable isomers of saturated polysilanes (Si_nH_{2m}), divalent silylenes ($Si_nH_{2m}B$), and double-bonded silenes ($Si_nH_{2m}A$) were considered. We refer the reader to Swihart and Girshick (1999a) for particular geometry of these molecules. For chemical reactions among small silicon hydride molecules (SiH_2, SiH_4, Si_2H_4A, Si_2H_4B, Si_2H_6, and Si_3H_8), pressure-dependent rate parameters and thermochemistry from Ho, Coltrin, and Brieland (1994) were used. For larger silicon hydride clusters, five types of generic reversible reactions were considered as shown in Table 1. The saturated polysilanes could either thermally decompose to silylenes by hydrogen elimination (reaction type R1) or to smaller saturated polysilanes by silylene elimination (reaction type R2). Silylenes can insert into silenes to form larger silenes (reverse of reaction type R3) or isomerize to form silenes with the same stoichiometry (reaction type R4). Isomerization of silylenes to polysilanes (with more than three silicon atoms) results in the formation of a ring (reaction type R5). For example, isomerization of linear $Si_5H_{10}B$ results in the formation of cyclic Si_5H_{10} with one ring, while isomerization of cyclic Si_5H_8B with one ring results in formation of cyclic Si_5H_8 with two rings. Ring formation plays a key role in the silicon hydride cluster growth, as once a silicon atom is incorporated into a ring, it cannot be eliminated from the cluster via reactions of type R2 or R3 without the ring first opening via reverse of reaction type R5. The thermochemistry and kinetics of these reactions were estimated based on known reactivity and thermodynamics of small silicon hydride molecules (see Swihart & Girshick, 1999a, for details). A recent study by Tonokura, Murasaki, and Koshi (2002) reported that the gas phase kinetic model simulations using the Swihart and Girshick model were qualitatively consistent with mass-spectrometric and photo-ionization measurements for silicon hydride cluster growth during disilane thermal decomposition.

In addition to the main collisionally stabilized channels for disilane and trisilane decomposition (reverse of reaction of type R1 and R2), Ho et al. (1994) also included the chemically activated channels for disilane and trisilane decomposition (Moffat, Jensen, & Carr, 1992; Becerra & Walsh, 1987)

$$SiH_2 + SiH_4 \rightleftharpoons Si_2H_6^* \rightleftharpoons Si_2H_4B + H_2, \tag{R6a}$$

$$SiH_2 + Si_2H_6 \rightleftharpoons Si_3H_8^* \rightleftharpoons Si_2H_4B + SiH_4. \tag{R6b}$$

These chemically activated pathways are especially important under low-pressure conditions, where the relative importance of the collisionally stabilized pathways is reduced (Moffat et al., 1992). The kinetics of chemically activated channels for larger silicon hydride clusters was not included in the model. However, it is expected that the relative importance of chemically activated channels will decrease as the number of degrees of freedom increases in larger molecules (Swihart & Girshick, 1999a).

In order to predict the measured film growth rates, the pre-exponential factors of R6a and R6b were reduced by a factor of 8 from the previously reported values (Ho et al., 1994; Moffat et al., 1992). Nijhawan (1999) reported that the kinetic mechanism of Ho et al. (1994) overpredicts the measured film growth rate by a factor of > 10 at deposition temperatures $> 700°C$ under low-pressure conditions. A detailed sensitivity analysis showed that the film growth rate is most sensitive to the rate of reaction of R6a, which results in the formation of Si_2H_4B, followed by isomerization to form the primary growth precursor Si_2H_4A (see also Section 4). Since the rate parameters of chemically activated channels are only known within roughly an order of magnitude (Moffat et al., 1992; Moffat, Swihart, & Nijhawan, 1998), the pre-exponentials of these reactions were reduced by a factor of 8 to get better agreement between the calculated and the observed film growth rates. Since the main difference between the measured and predicted film growth rates was at high-deposition temperatures ($> 700°C$), it is likely that other temperature-dependent uncertainties exist in the rate parameters of reactions R6a and R6b.

The reversible silicon hydride clustering growth/decay mechanism was terminated at clusters containing ten silicon atoms. Larger clusters containing eleven, twelve, and thirteen silicon atoms were allowed to form irreversibly by the reverse of reactions of type R2 and R3. This switchover from reversible to irreversible cluster growth corresponds to the size of particle nuclei with rate of formation (or nucleation rate), J, given by

$$J = \frac{\alpha}{2} \sum_{g^*=11}^{13} \sum_{k=1}^{g^*-1} \beta_{k,g^*-k} n_k n_{g*-k}. \tag{1}$$

In Eq. (1), $\beta_{k,j}$ is the bimolecular collision rate (with no activation energy) between clusters of size k and j, n_k is the total number concentration of silicon hydride clusters containing k silicon atoms, and α is an arbitrary constant that was used to simulate the effect of other kinetic bottlenecks in the chemical clustering mechanism as discussed in Section 4. Note that only interactions between clusters that follow the chemical reaction rules listed in Table 1 were considered in Eq. (1). Furthermore, in evaluating the nucleation rate no distinction is made between species based on the number of hydrogen atoms. Such a formulation was needed because we do not attempt to calculate composition or structure for particles that contain more than 10 silicon atoms.

3.2. Heterogeneous film and particle growth model

We use the surface kinetics mechanism presented by Ho et al. (1994) to model particle growth. The model includes dual-site dissociative adsorption of saturated polysilanes (Houf, Grcar, & Breiland, 1993; Ho et al., 1994), followed by hydrogen desorption from the surface (Sinniah et al., 1989, 1990) as shown in Table 2. Following the work of Buss et al. (1988) the rate parameters for saturated polysilanes were set to 10 times the reaction rate of silane. A sensitivity study showed that

Table 2
Summary of surface reactions and rate parameters (Ho et al., 1994) used in this study. The kinetic parameters are given in units of moles, cm, s, cal, and K. The hydrogen desorption reaction exhibits first-order kinetics in SiH(S) coverage (Sinniah et al., 1989, 1990).

Reaction type	General form	A	E_{act}
Silane adsorption	$SiH_4 + 2Si(S) \rightarrow 2SiH(S) + Si(B) + H_2$	8.39×10^{26}	37450.0
Saturated polysilane adsorption ($n \geqslant 2$)	$Si_nH_{2m} + 2Si(S) \rightarrow 2SiH(S) + nSi(B) + (m-1)H_2$	8.39×10^{27}	37450.0
Hydrogen desorption	$2SiH(S) \rightarrow 2Si(S) + H_2$	1.75×10^{20}	47000.0
Silylene adsorption	$Si_nH_{2m}B \rightarrow nSi(B) + mH_2$	1.0[a]	0.0
Silene adsorption	$Si_nH_{2m}A \rightarrow nSi(B) + mH_2$	1.0[a]	0.0

[a]Surface reaction sticking probability.

the particle and film growth rates were most sensitive to the heterogeneous hydrogen desorbtion as roughly 80% of silicon sites were occupied by hydrogen under the conditions examined (Nijhawan, 1999). The film and particle growth rates were not sensitive to rate parameters for the surface reaction of silylenes and silenes, which were assumed to have unit surface sticking probabilities.

It should be noted that the surface kinetics model of Ho et al. (1994) is a bulk film growth model. The use of the model is a reasonable approximation for particles greater than a few nanometers in size as the particle surface is essentially bulk to molecular clusters, but an imperfect approximation when applied to particles as small as nuclei, which in our case contain only 11–13 silicon atoms. Another novel aspect of this work was incorporation of temperature-dependent surface kinetics in the particle growth model. This required the solution of temperature-dependent surface species site conservation equations to obtain the concentration of surface species on particle surfaces (Nijhawan, 1999). Furthermore, species mass-conservation equations were modified with terms to account for species depletion due to particle growth by surface reactions (Nijhawan, 1999).

3.3. *Fully and quasi-coupled solution algorithms*

Numerical results using fully and quasi-coupled formulations are presented in this work. These formulations are schematically shown in Fig. 3. In both formulations, first the governing equations are simultaneously solved by neglecting the numerically stiff particle growth/depletion and coagulation terms. This gives spatial profiles of velocity, temperature, and concentrations of mass-conserved chemical species and nuclei. Using this solution as the initial guess, the governing equations with all the terms are solved in the fully coupled formulation, whereas in the quasi-coupled formulation only particle moment equations are solved by considering nuclei formation/depletion and heterogeneous particle growth. That is, in the quasi-coupled formulation the heterogeneous growth species depletion and coagulation are neglected. We show later in Section 4 that both fully and quasi-coupled models are in qualitative agreement with the measurements when less than 1% of the total silicon mass in the gas resides in the particles. Under these low-particle mass loading conditions (process pressure $\leqslant 2.5$ Torr and temperature $\leqslant 750°C$), a quasi-coupled solution is of practical importance as it can be obtained in $\sim$20 min of real time. In comparison, the fully coupled solution requires $\sim$15 h of real time on the IBM SP supercomputer.

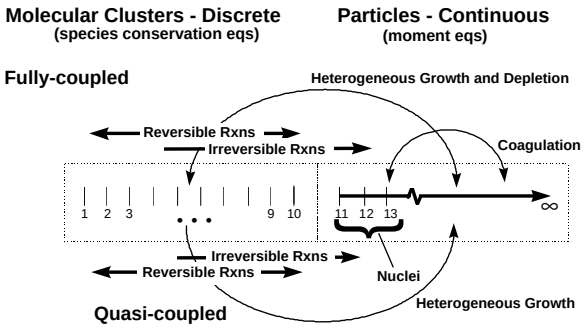

Fig. 3. Schematic representation of the fully and quasi-coupled formulations.

4. Results and discussion

The calculated axial profiles for gas-phase species concentrations, dominant clustering pathways, and resulting particle concentration and growth rate for the base case conditions (100% silane at 2.0 Torr, 750°C wafer temperature) listed in Table 3 are shown in Figs. 4 and 5. In these fully coupled simulations, depletion of particle nucleation precursors, depletion of heterogeneous film and particle growth precursors, coagulation, and transport were included.

Fig. 4a shows axial profiles for species with concentrations exceeding 10^9 cm^{-3}. At these conditions, only 3% of the SiH_4 mass introduced at the showerhead inlet dissociates to form H_2 and SiH_2. Since reactive-divalent SiH_2 inserts in SiH_4 to form larger clusters, its concentration is considerably lower than the hydrogen concentration. Dominant polysilane species include Si_2H_6 and Si_3H_8, followed by Si_4H_8, Si_4H_{10}, Si_5H_{10}, and Si_3H_6. Also, silenes are produced in higher concentrations than their silylene isomers. Among the silenes, the concentrations of Si_2H_4A and Si_5H_6A are highest ($\sim 10^{12}$ cm^{-3}), followed by Si_4H_6A, Si_3H_6A, and Si_3H_4A. Formation of silenes is especially important, as they are predicted to be the primary heterogeneous (particle and film) growth precursors as shown in Fig. 4b. This is because these species are highly reactive with unit surface reaction sticking probability in our model. In comparison, saturated polysilanes were assumed to have an activation energy of 37.5 kcal/mol for reaction on silicon surfaces. As a result, even though silane concentrations exceed those of Si_2H_4A and Si_5H_6A by four orders of magnitude (Fig. 4a), silane only contributes 3% to the maximum total growth rate, while Si_2H_4A and Si_5H_6A contribute 77% and 18% to the maximum total growth rate, respectively. The results in Fig. 4b also show that film

Table 3
Summary of the base case process parameters.

Process Parameter	
Silane mass flow, Q_{inlet} (sccm)	200.0
Pressure, P (torr)	2.0
Wafer temperature, T_{wafer}(°C)	750.0
Inlet temperature, T_{inlet}(°C)	200.0[a]

[a]Determined experimentally.

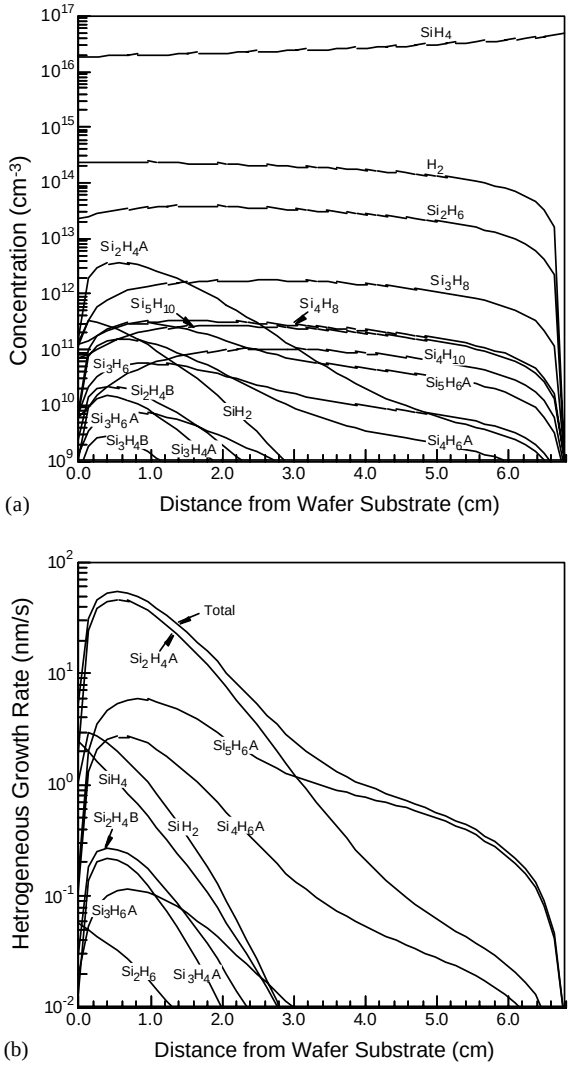

Fig. 4. Predicted (a) species concentrations and (b) heterogeneous growth rate profiles at the base case conditions listed in Table 3.

growth rates at the wafer are roughly a factor of 10 lower than the maximum particle growth rates. This is because the total surface area of the film is a factor of $\sim 10^2$ greater than the predicted total particle surface area in the reactor at these conditions, which results in considerable growth species depletion at the wafer and the observed maximum in the growth rate profiles in Fig. 4b.

The spatial profiles of predicted total particle concentration are shown in Fig. 5a. A comparison of predicted particle concentration and diameter with measurement at the base case conditions indicates that the fully coupled model (with $\alpha = 1$) overpredicts the measured particle concentrations ($\sim 10^5$ cm^{-3}) by a factor of 10^4 (Nijhawan, 1999; Fig. 6b). The large discrepancy in particle concentration suggests that other kinetic bottlenecks for clusters containing more than 10 silicon atoms,

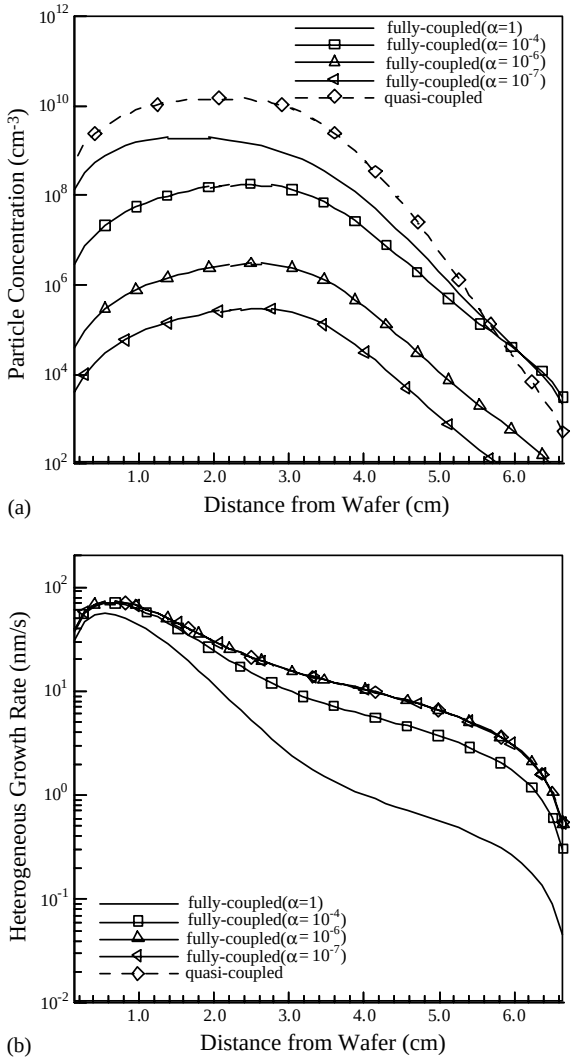

Fig. 5. Predicted (a) particle concentration and (b) heterogeneous growth rate at base case conditions listed in Table 3 for different values of α (Eq. (1)).

which we have not accounted for in our formulation, exist in the chemical clustering mechanism. Including other bottlenecks in the chemical clustering mechanism would lower the predicted particle nucleation rate and concentration. To simulate the effect of other kinetic bottlenecks numerical simulations were performed at the base case conditions by arbitrarily reducing the number of effective collisions in Eq. (1) by a constant factor, α, as shown in Fig. 5. In the fully coupled model, with the reduced effective collision rate the predicted particle concentrations decrease (Fig. 5a). The reduced particle concentration in turn increases the particle growth precursor concentration in the gas phase, which in turn increases the heterogeneous particle growth rate as shown in Fig. 5b. Note that due to coupling between nuclei formation and species depletion, decreasing the number of effective

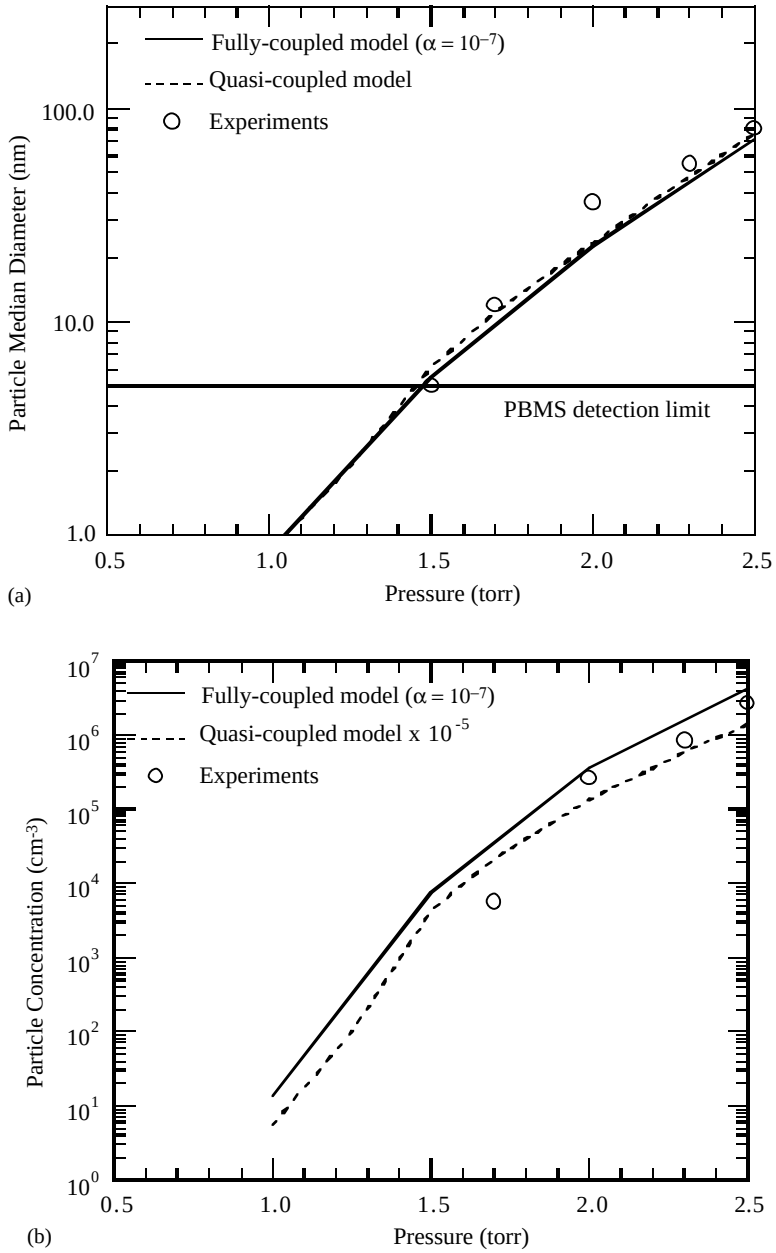

Fig. 6. Effect of process pressure on: (a) particle median diameter and (b) concentration for inlet silane mass flow rate of 200 sccm and wafer temperature of 750°C.

collisions by factor of 10^7 only reduces the maximum particle nucleation rate and concentration by a factor of 10^4. As shown in Fig. 5a, $\alpha = 10^{-7}$ was needed to obtain predicted particle concentrations of 10^5 cm^{-3}, which were in approximate quantitative agreement with the measurements as noted later.

The numerical results in Fig. 5b also suggest that for low-particle mass loadings, particle nucleation and growth are decoupled. This is because under these conditions the depletion of heterogeneous growth precursors and coagulation are unimportant, and thus both fully and quasi-coupled models predict the same particle growth rates as shown in Fig. 5b. This is of considerable practical importance as a computationally cheap quasi-coupled formulation would be adequate under these low-particle-loading conditions as shown later.

Figs. 6–9 show the results of measurements obtained using the capillary probe shown in Fig. 1. In these measurements, the total current detected by the PBMS was recorded as the capillary probe was transported axially at a radial location corresponding approximately to the radius of the substrate assembly. Complete size distributions were measured only at the point where the total particle current (proportional to the product of total particle concentration and mean number diameter) reached its maximum value. Therefore, the results of the numerical model are compared with measurements at this point.

Figs. 6a and b show the measured and predicted particle number-median diameter and concentration as a function of process pressure. Numerical results for both the quasi-coupled and fully coupled models are shown. Note that even though the quasi-coupled model overpredicts the measured particle concentration by a factor of 10^5, it correctly predicts the relative increase in the total particle concentration with gas pressure. The results show that $\alpha = 10^{-7}$ was needed to predict the measured particle concentrations in the fully coupled simulations. Also, both the quasi-coupled and fully coupled model accurately predict the measured particle sizes. This is because under these conditions less than 0.1% of the silicon mass introduced at the inlet resides in the particles, and depletion of particle growth species is unimportant.

The numerical results can also be used to estimate the critical pressure for particle formation. We define the critical pressure as the value above which the calculated median particle diameter exceeds 0.005 μm. We used this value because the PBMS does not detect particles smaller than this size. Both quasi-coupled and fully coupled models predict a critical pressure of 1.4 Torr, which is in very good agreement with the measured value of 1.5 Torr (Nijhawan, 1999).

Figs. 7a and b show the variation of particle concentration and median diameter with wafer temperature. It is seen that at deposition temperatures greater than 775°C, the depletion of particle growth species is important, and a fully coupled model is needed to predict the experimental observations. Consistent with the previous results, the quasi-coupled model predicts the measured particle diameter and relative concentration for low-particle mass loading conditions (deposition temperature $\leqslant 750$°C). Also, note that the predicted critical temperature of 720°C is in good agreement with the experimentally determined value of 715°C (Nijhawan, 1999).

We have previously reported that at low pressures in a parallel-plate reactor geometry the particles are confined in a thin sheath between the "hot" wafer and the "cold" showerhead inlet (Nijhawan, McMurry, & Campbell, 2000). This sheath is located at the point where downward convective transport balances upward transport by thermophoresis. The effect of inlet mass flow rate and pressure on the location of this particle sheath are shown in Fig. 8. The vertical bars in the figure indicate the full-width at half-maximum of the predicted and measured particle current profiles. The quasi-coupled model predicts the overall features observed in the measurements. Decreasing the silane mass flow rate (at fixed pressure and temperature) moves the particle sheath toward the showerhead inlet. Furthermore, at fixed inlet mass flow rate and temperature the ratio of the convective flow velocity and thermophoretic particle velocity does not change, which in turn does not change the location of

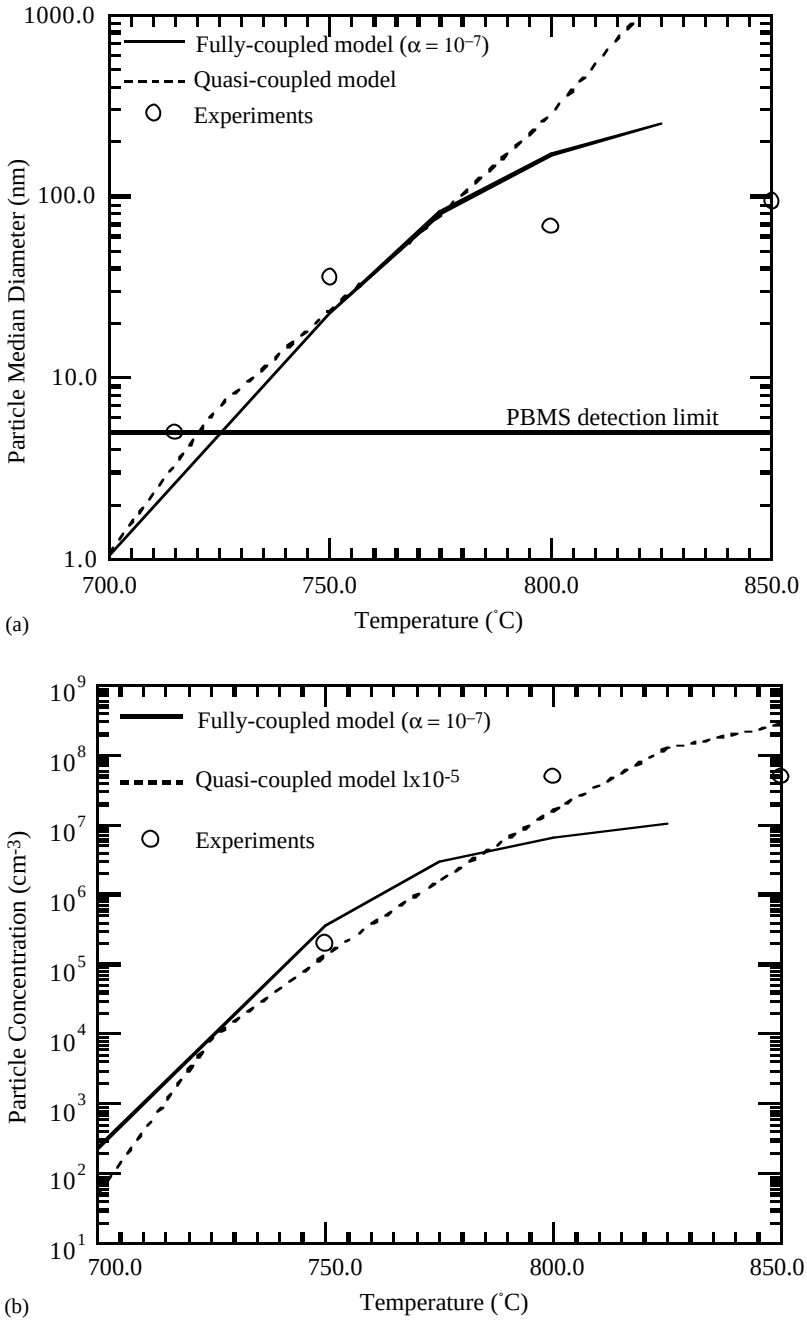

Fig. 7. Effect of wafer temperature on: (a) particle median diameter and (b) concentration for process pressure of 2.0 Torr and inlet silane mass flow rate of 200 sccm.

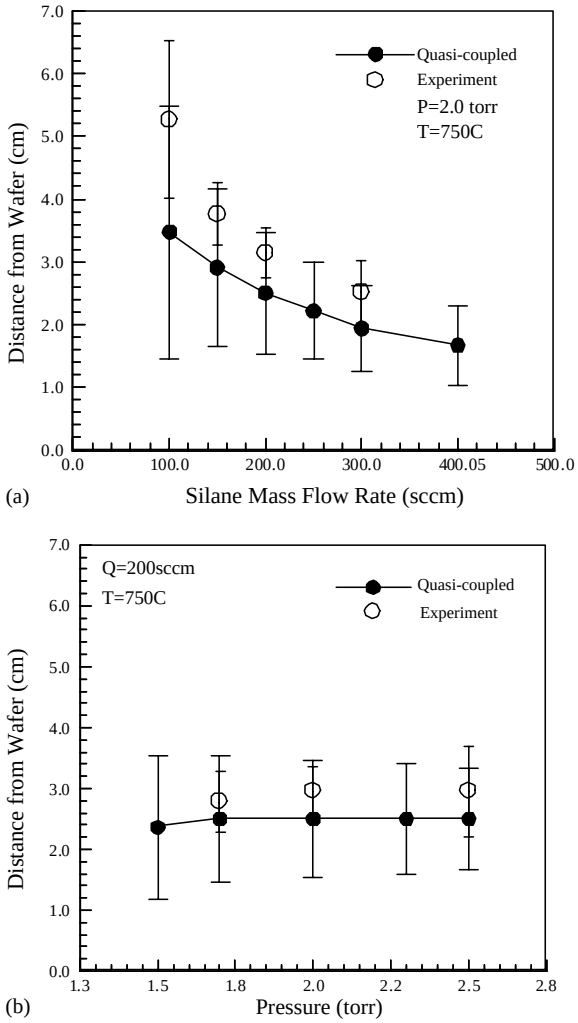

Fig. 8. Effect of (a) inlet mass flow rate and (b) pressure on predicted and measured location of the particle layer. The vertical bars indicate the full width at half maximum of particle layer profiles.

the particle sheath as seen in Fig. 8b. However, note that the model predicts a considerably thicker particle layer than was observed experimentally.

Fig. 9 shows the effect of addition of nitrogen and hydrogen on particle formation at fixed total gas pressure (2.0 and 2.5 Torr), fixed temperature (750°C), and fixed total inlet silane and diluent flow rate (200 sccm). The results show that with the decrease in silane volume fraction both particle median diameter and concentrations decrease. This is expected as decreasing the silane volume fraction at total fixed pressure and residence time is equivalent to decreasing the partial pressure of silane, which in turn slows the particle nucleation and growth kinetics. Furthermore, the results show that hydrogen is more effective in suppressing particle formation than nitrogen. This is because hydrogen is formed as a product during thermal pyrolysis. Thus, addition of hydrogen will suppress

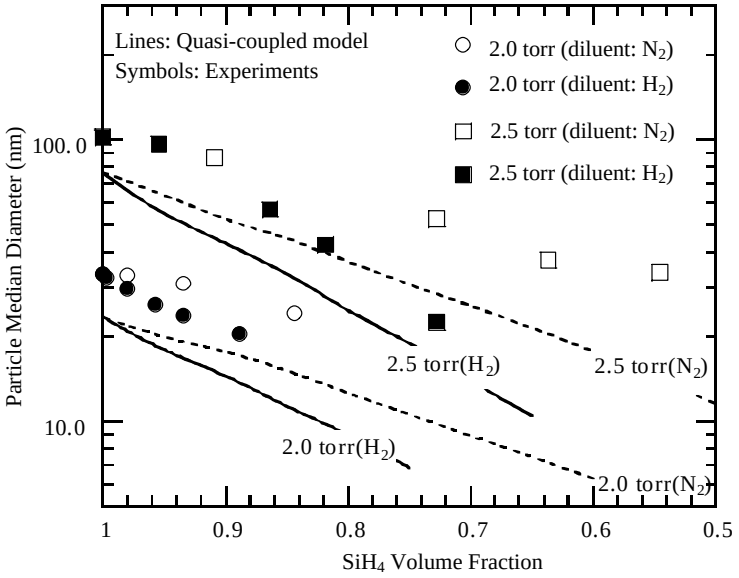

Fig. 9. Effect of diluent gas on particle median diameter at wafer temperature of 750°C and total (silane and diluent) mass flow rate of 200 sccm.

thermal decomposition of silane, which in turn retards the particle nucleation and growth kinetics. Also, addition of hydrogen favors formation of silicon hydride clusters with lower silicon-to-hydrogen ratio (less ring formation), which in turn suppresses particle nucleation.

The predicted and measured critical pressure and temperature for particle formation are shown in Fig. 10, where we also compare our results with other experimental studies reported in the literature. These include low-pressure experiments of Qian, Michiel, Ammel, Nijs, and Mertens (1988) and atmospheric-pressure experiments of Eversteijn (1971), Murthy, Miyamoto, Shimbo, and Nishizawa (1976), and Slootman and Parent (1994). Also, the pressure and temperature at which particle formation occurs is estimated using fully coupled formulation based on a 0.005 μm particle size threshold to permit comparison with the PBMS measurements.

As seen in Fig. 10, our measurements are in good agreement with the low-pressure study of Qian et al. (1988). We measure an activation energy of 12.6 kcal/mol for particle formation, which is in close agreement with the activation energy of 8 kcal/mol reported by Qian et al. (1988). The slight difference in these measured values is attributed to differences in the reactor geometry (showerhead vs. tubular reactor) and measurement techniques (PBMS vs visual) used in the two studies. Also, the predicted activation energy of ~18.5 kcal/mol for particle formation is in reasonable agreement with our measured value of 12.6 kcal/mol. The primary difference between the predicted and measured values is for deposition temperatures greater than 775°C. As shown in Figs. 6 and 7 both quasi-coupled and fully coupled models predict the same critical temperature and pressures. As a result, we attribute this inconsistency to the uncertainty in the temperature-dependent reaction rates of collisionally stabilized reactions, R6a and R6b, which play an important role in formation of primary growth precursor disilane (see also Section 3). Additional work is needed in the future to

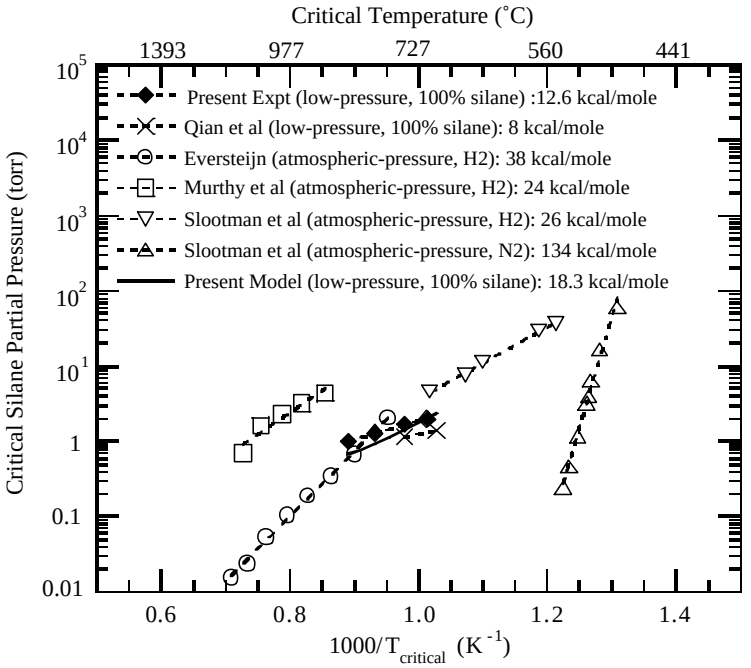

Fig. 10. Comparison of critical pressure and temperature for particle formation reported in this work with available data in the literature. The figure label also shows the activation energy of particle formation.

obtain better estimates of the reaction rates of these chemically activated channels in the chemical clustering mechanism.

In contrast, in atmospheric-pressure thermal decomposition of silane considerably higher activation energies (24–38 kcal/mol with hydrogen carrier gas and 134–145 kcal/mol with inert carrier gases) have been reported (Fig. 10). In addition, note that the magnitudes of the critical pressure for particle formation in low-pressure studies are in better agreement with atmospheric pressure studies with hydrogen rather than nitrogen as carrier gas, as shown in Fig. 10. This is due to the fact that the presence of hydrogen as carrier gas suppresses thermal decomposition of silane. As a result, we expect the formation of Si_2H_4A and Si_2H_4B (rate limiting steps during low-pressure conditions) to also play an important role during particle formation under atmospheric conditions in hydrogen. In contrast, an activation energy of 130–150 kcal/mol has been reported at atmospheric pressures during silane pyrolysis with inert carrier gases (Fig. 10), which is indicative of other rate limiting steps.

The ability to predict "particle-free" process space is a useful engineering tool for semiconductor process design and contamination control. As shown in this work the quasi-coupled approach can be used to predict observations for the pressure and temperature at which particle formation begins. Therefore, the computationally inexpensive quasi-coupled formulation is suggested as an engineering tool for semiconductor equipment design and contamination control during thermal silicon deposition. The work also highlights the need for better understanding of gas phase kinetics of chemically activated reactions (R6) and surface reaction kinetics of disilane as they may play a critical role in particle formation and growth in low-pressure CVD conditions.

5. Conclusions

An aerosol dynamics moment-type model coupled with a chemically reacting fluid flow model was used to predict particle concentration and size in the stagnation flow region of a parallel-plate CVD reactor. Relevant processes such as nucleation via a sequence of chemical clustering reactions, particle growth by heterogeneous chemical reactions and coagulation, and transport were included in the model. This approach was used to identify the dominant chemical clustering pathways and rate limiting kinetic bottlenecks that lead to formation of particle nuclei. The numerical results show several pathways involving linear and polycyclic silicon hydride molecules result in formation of the particle "nuclei," which subsequently grow by heterogeneous reaction of disilane on the particle surfaces. It is shown that under conditions of low-particle mass loadings (deposition temperatures $\leqslant 750\ ^{\circ}C$ and process pressures $\leqslant 2.5$ Torr), depletion of growth precursors and coagulation is unimportant. This is of considerable practical importance as neglecting these numerically stiff terms in a quasi-coupled formulation reduces the computation cost by two orders of magnitude. Overall the model is in good agreement with observations for the pressure and temperature at which particle formation begins, particle sizes and growth rates, and relative particle concentrations at various process conditions. We suggest the computationally inexpensive quasi-coupled model as an engineering tool for process reactor design and contamination control during low-pressure silicon deposition.

Acknowledgements

The authors thank Dr. Pauline Ho at Sandia National Laboratories (SNL) for helpful discussions on the role of cyclic molecules on particle formation. We also acknowledge the help of Dr. Harry K. Moffat at SNL for modifications to the SPIN code. This research was partially supported by Semiconductor Research Corporation under contract SRC/97-BJ-442, by the Sandia National Laboratories under contract DE-AC04-94AL85000, and by the National Science Foundation under Grant CTS-9909563. Modeling work was supported by a research grant from the Minnesota Supercomputer Institute. Sandeep Nijhawan was also supported during this research by a fellowship from the Graduate School of the University of Minnesota.

References

Allen, K. D., & Sawin, H. H. (1986). Thermodynamics of the silicon–chlorine–hydrogen system: Chemical potential for homogeneous nucleation. *Journal of Electrochemicals*, *133*(2), 421–425.

Becerra, R., & Walsh, R. (1987). Mechanism of formation tri- and tetrasilane in the reaction of atomic hydrogen with monosilane and the thermochemistry of Si2H4 isomers. *Journal of Physical Chemistry*, *91*, 5765–5770.

Brekel, C. H. vandenJ., & Bollen, L. J. M. (1981). Low pressure deposition of polycrystalline silicon from silane. *Journal of Crystal Growth*, *54*, 310–322.

Buss, R. J., Ho, P., Breiland, W. G., & Coltrin, M. E. (1988). Reactive sticking coefficients for silane and disilane on polycrystalline silicon. *Journal of Applied Physics*, *63*(8), 2808–2818.

Chiu, C.-P. (1992). *Modeling thermal plasma synthesis of fine powders*. Ph.D. Thesis, University of Minnesota.

Claassen, W. A. P., Bloem, J., Valkenburg, W. G. J. N., & van den Brekel, C. H. J. (1982). The deposition of silicon from silane in low-pressure hot-wall system. *Journal of Crystal Growth*, *57*, 259–266.

Coltrin, M.E., Kee, R.J., Evans, G.H., Meeks, E., Rupley, F.M., & Grcar, J.F. (1991). SPIN (verison 3.83): A FORTRAN package for modeling one-dimensional rotating-disk/stagnation-flow chemical vapor deposition reactors, Sandia National Laboratory Report, SAND91-8003.UC-401.

Coltrin, M. E., Kee, R. J., & Miller, J. A. (1986). A mathematical model of silicon chemical vapor deposition. *Journal of Electrochemical Society*, *133*(6), 1206–1213.

Coltrin, M.E., Kee, R.J., Rupley, F.M., & Meeks, E. (1996). SURFACE CHEMKIN-III: A FORTRAN package for analyzing heterogeneous chemical kinetics at a solid-surface–gas-phase interface, Sandia National Laboratory Report, SAND96-8217.

Comfort, J. H., & Reif, R. (1989). Chemical vapor deposition of epitaxial silicon from silane at low temperature. *Journal of Electrochemical Society*, *136*(8), 2386–2398.

Donahue, T. J., & Reif, R. (1986). Low temperature silicon epitaxy deposited by low pressure chemical vapor deposition. *Journal of Electrochemical Society*, *133*(8), 1691–1697.

Epstein, P. S. (1924). On the resistance experienced by spheres in their motion through gases. *Physics Review*, *23*, 710–733.

Eversteijn, F. C. (1971). Gas-phase decomposition of silane in horizontal epitaxial reactor. *Phillips Research Reports*, *26*, 134–144.

Flint, J. H., Marra, R. A., & Haggerty, J. S. (1986). Powder temperature, size, and number density in laser driven reactions. *Aerosol Science Technology*, *5*, 249–260.

Foster, D. W., Learn, A. J., & Kamins, T. I. (1986). Deposition properties of silicon films formed from silane in a vertical-flow reactor. *Journal of Vacuum Science and Technology B*, *4*(5), 1182–1186.

Frenklach, M., Ting, L., Wang, H., & Rabinowitz, M. (1996). Silicon particle formation in pyrolysis of silane and disilane. *Israel Journal of Chemistry*, *36*, 293–303.

Girshick, S. L., Swihart, M. T., Suh, S. -M., Mahajan, M. R., & Nijhawan, S. (2000). Numerical modeling of gas-phase nucleation and particle growth during chemical vapor deposition of silicon. *Journal of Electrochemical Society*, *147*(6), 2303–2311.

Giunta, C. J., McCurdy, R. J., Chapple-Sokol, J. D., & Gordon, R. G. (1990). Gas-phase kinetics in the atmospheric pressure chemical vapor deposition of silicon from silane and disilane. *Journal of Applied Physics*, *67*(2), 1062–1075.

O'Hanlon, J. F., & Parks, H. G. (1992). Impact of vacuum contamination on semiconductor yield. *Journal of Vacuum Science and Technology A*, *10*(4), 1863–1868.

Hargis, P. J., Greenberg, K. E., Miller, P. A., Gerado, J. B., et al. (1994). The Gaseous Electronic Conference radio-frequency reference cell: A defined parallel plate radio frequency system for experimental and theoretical studies of plasma processing discharges. *Review of Scientific Instruments*, *65*, 140–154.

Hattori, T. (1990). Contamination control: Problems and prospects. *Solid State Technology*, *33*(7), S1.

Herrick, C. S., & Martinez, R. A. S. (1984a). Equilibrium calculations for the Si–H–Cl system from 300 to 3000 K. *Journal of Electrochemical Society*, *131*(2), 455–458.

Herrick, C. S., & Woodruff, D. W. (1984b). The homogeneous nucleation of condensed silicon in the gaseous Si–H–Cl system. *Journal of Electrochemical Society*, *131*(10), 2417–2422.

Ho, P., Coltrin, M. E., & Brieland, W. G. (1994). Laser-induced fluorescence measurements and kinetic analysis of Si atom formation in rotating disk chemical vapor deposition reactor. *Journal of Physical Chemistry*, *98*, 10138–10147.

Ho, P., Nijhawan, S., & Brockmann, J.E. (1996). Private communication.

Houf, W. G., Grcar, J. F., & Breiland, W. G. (1993). A model for low pressure chemical vapor deposition in hot-wall tubular reactor. *Material Science Engineering*, *B17*, 163–171.

Joyce, B. A., & Bradley, R. R. (1963). Epitaxial growth of silicon from the pyrolysis of monosilane on silicon substrates. *Journal of Electrochemical Society*, *110*(12), 1235–1240.

Kee, R.J., Rupley, F.M., Meeks, E., & Miller, J.A. (1996). CHEMKIN-III: A FORTRAN chemical kinetics package for the analysis of gas-phase chemical and plasma kinetics. Sandia National Laboratory Report, SAND96-8216.UC-405.

Kelkar, M., Rao, N.P., & Girshick, S.L. (1996). Homogeneous nucleation of silicon: Effect of the properties of kinetics of small clusters. In M. Kulmala, & P.W. Wagner (Eds.), *Proceedings of the 14th International conference on nucleation and atmospheric aerosols*, Helsinki, Finaland August 26–30, Pergamon, pp. 117–120.

Kruis, F. E., Schoonman, J., & Scarlett, B. (1994). Homogeneous nucleation of silicon. *Journal of Aerosol Science*, *25*(7), 1291–1304.

Liu, P., Ziemann, P. J., Kittelson, D. B., & McMurry, P. H. (1995a). Generating particle beams of controlled dimensions and divergence. I. Theory of particle motion in aerodynamic lenses and nozzle expansions. *Aerosol Science Technology*, *22*, 293–313.

Liu, P., Ziemann, P. J., Kittelson, D. B., & McMurry, P. H. (1995b). Generating particle beams of controlled dimensions and divergence. II. Experimental evaluation of particle motion in aerodynamic lenses and nozzle expansions. *Aerosol Science Technology*, *22*, 314–324.

McMurry, P. H., Nijhawan, S., Rao, N. P., Ziemann, P. J., Kittelson, D. B., & Campbell, S. A. (1996). Particle beam mass spectrometer measurements of particle formation during low pressure chemical vapor deposition of polysilicon and SiO_2 films. *Journal of Vacuum Science and Technology A*, *14*(2), 582–587.

Moffat, H. K., Jensen, K. F., & Carr, R. W. (1992). Estimation of Arrhenius parameters for the 1,1 of H_2 from Si_2H_6 and the chemically activated disilane in silane pyrolysis. *Journal of Physical Chemistry*, *96*, 7695–7703.

Moffat, H.K., Swihart, M.T., & Nijhawan, S. (1998). Private communication.

Murthy, T. U. M. S., Miyamoto, N. M., Shimbo, M., & Nishizawa, J. (1976). Gas-phase nucleation during thermal decomposition of silane in hydrogen. *Journal of Crystal Growth*, *33*, 1–7.

Nijhawan, S. (1999). *Experimental and computational study of particle nucleation, growth, and transport during low-pressure thermal decomposition of silane*. Ph.D. Thesis, University of Minnesota.

Nijhawan, S., McMurry, P.H., & Campbell, S.A. (2000). Particle transport in a parallel-plate semiconductor reactor: Chamber modification and design criterion for enhanced process cleanliness. *Journal of Vacuum Science and Technology A*, *18*, 2198–2206.

Nijhawan, S., Rao, N.P., Kittelson, D.B., McMurry, P.H., Campbell, S.A., Brockmann, J.E., & Geller, A.S. (1998). Particle measurements and transport in silane LPCVD. *Proceedings of the 44th annual conference of the institute of environmental sciences*, Phoenix, AZ.

Onischuk, A. A., Strunin, V. P., Samoilova, R. I., Nosov, A. V., Ushakova, M. A., & Panfilov, V. N. (1997a). Chemical composition and bond structure of aerosol particles of amorphous hydrogenated silicon forming from thermal decomposition of silane. *Journal of Aerosol Science*, *28*(8), 1425–1441.

Onischuk, A. A., Strunin, V. P., Ushakova, M. A., & Panfilov, V. N. (1994). Analysis of hydrogen in aerosol particles of a-Si:H forming during the pyrolysis of silane. *Physical Status Solid B*, *186*, 43–55.

Onischuk, A. A., Strunin, V. P., Ushakova, M. A., & Panfilov, V. N. (1997b). On the pathways of aerosol formation by thermal decomposition of silane. *Journal of Aerosol Science*, *28*(2), 207–222.

Phanse, G. M., & Pratsinis, S. E. (1989). Theory of aerosol generation in laminar flow condensers. *Aerosol Science Technology*, *11*, 100–119.

Pratsinis, S. E., & Kim, K.-S. (1989). Particle coagulation, diffusion, and thermophoresis in laminar flows. *Journal of Aerosol Science*, *20*(1), 101–111.

Purnell, J. H., & Walsh, R. (1966). The pyrolysis of monosilane. *Proceedings of the Royal Society A*, *293*, 543–561.

Qian, Z. M., Michiel, H., Ammel, A. V., Nijs, J., & Mertens, R. (1988). Homogeneous gas phase nucleation of silane in low pressure chemical vapor deposition (LPCVD). *Journal of Electrochemical Society*, *135*, 2378–2379.

Rao, N. P., Nijhawan, S., Kim, T., Wu, Z., Campbell, S. A., Kittelson, D. B., McMurry, P. H., Cheng, C. C., & Mastromatteo, E. (1998a). Investigation of particle generation during the low pressure chemical vapor deposition of Borophosphosilicate glass films. *Journal of Electrochemical Society*, *145*, 2051–2057.

Rao, N. P., Wu, Z., Nijhawan, S., Ziemann, P. J., Campbell, S. A., Kittelson, D. B., & McMurry, P. H. (1998b). Investigation of particle generation during the plasma enhanced chemical vapor deposition of amorphous silicon, oxide, and nitride films. *Journal of Vacuum Science and Technology B*, *16*(2), 483–489.

Sinniah, K., Sherman, M. G., Lewis, L. B., Henry Weinberg, W., Yates, J. T., & Janda, K. C. (1989). New mechanism for hydrogen desorption from covalent surfaces: The monohydride phase on Si(100). *Physics Review Letters*, *62*(5), 567–570.

Sinniah, K., Sherman, M. G., Lewis, L. B., Weinberg, W. H., Yates, J. T., & Janda, K. C. (1990). Hydrogen desorption from the monohydride phase on Si(100). *Journal Chemical Physics*, *92*(9), 5700–5711.

Sladek, K. J. (1971). The role of homogeneous reactions in chemical vapor deposition. *Journal of Electrochemical Society*, *118*(4), 654–657.

Slootman, F., & Parent, J. C. (1994). Homogeneous gas-phase nucleation in silane pyrolysis. *Journal of Aerosol Science*, *25*(1), 15–21.

Swihart, M. T., & Girshick, S. L. (1999a). Thermochemistry and kinetics of silicon hydride cluster formation during thermal decomposition of silane. *Journal of Physical Chemistry*, *103B*, 64–73.

Swihart, M. T., & Girshick, S. L. (1999b). Ab initio structures and energetics of selected hydrogenated silicon clusters containing six to ten silicon atoms. *Chemical Physics Letters*, *307*, 527–532.

Tonokura, K., Murasaki, T., & Koshi, M. (2002). Formation mechanism of hydrogenated silicon clusters during thermal decomposition of disilane. *Journal of Physical Chemistry B*, *106*, 555–563.

Whitby, E.R. (1990). *Modal aerosol dynamics modeling*. Ph.D. Thesis, University of Minnesota.

White, R. T., Espino-Rios, R. L., Rogers, D. S., Ring, M. A., & O'Neal, H. E. (1985). Mechanism of silane decomposition. I. Silane loss of kinetics and rate inhibition by hydrogen. II. Modeling of the silane decomposition (all stages of the reaction). *International Journal of Chemical kinetics*, *17*, 1029–1065.

Veprek, S., Schopper, K., Ambacher, O., Rieger, W., & Veprek-Heijman, M. G. J. (1993). Mechanism of cluster formation in a clean silane discharge. *Journal of Electrochemical Society*, *140*(7), 1935–1941.

Yuuki, A., Matsui, Y., & Tachibana, K. (1987). A numerical study of gaseous reactions in silane pyrolysis. *Japanese Journal of Applied Physics*, *26*(5), 747–754.

Ziemann, P. J., Kittelson, D. B., & McMurry, P. H. (1996). Effects of particle shape and chemical composition on the electron impact charging properties of submicron inorganic particles. *Journal of Aerosol Science*, *27*(4), 587–606.

Ziemann, P. J., Liu, P., Nijhawan, S., Kittelson, D. B., McMurry, P. H., & Campbell, S. A. (1995b). Particle beam mass spectrometry of submicron particles formed during LPCVD of polysilicon films, *Proceedings of the 41st annual conference of the institute of environmental sciences*, Anaheim, CA, pp. 22–29.

Ziemann, P. J., Liu, P., Rao, N. P., Kittelson, D. B., & McMurry, P. H. (1995a). Particle beam mass spectrometry of particles charged to saturation in an electron beam. *Journal Aerosol Science*, *26*(5), 745–756.